Article

Crystal Structure and Growth Mechanism of Unusually Long Fullerene (C) Nanowires

Junfeng Geng, Wuzong Zhou, Paul Skelton, Wenbo Yue, Ian A. Kinloch, Alan H. Windle, and Brian F. G. Johnson

J. Am. Chem. Soc., **2008**, 130 (8), 2527-2534 • DOI: 10.1021/ja076392s

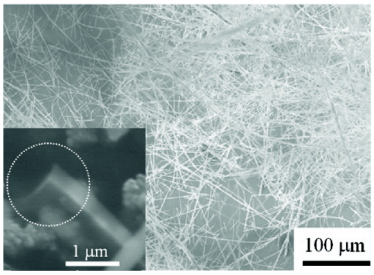

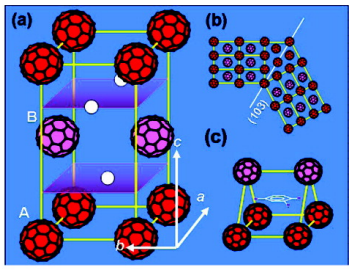

More About This Article

Additional resources and features associated with this article are available within the HTML version:

- Supporting Information
- Links to the 1 articles that cite this article, as of the time of this article download
- Access to high resolution figures
- Links to articles and content related to this article
- Copyright permission to reproduce figures and/or text from this article

View the Full Text HTML

J|A|C|S
ARTICLES
Published on Web 02/02/2008

Crystal Structure and Growth Mechanism of Unusually Long Fullerene (C_{60}) Nanowires

Junfeng Geng,*,† Wuzong Zhou,*,‡ Paul Skelton,† Wenbo Yue,‡ Ian A. Kinloch,§ Alan H. Windle,§ and Brian F. G. Johnson*,†

Department of Chemistry, University of Cambridge, Cambridge, CB2, 1EW, U.K., School of Chemistry, University of St. Andrews, St. Andrew, Fife KY16, 9ST, U.K., and Department of Materials Science and Metallurgy, University of Cambridge, CB2, 3QZ, U.K.

Received August 24, 2007; E-mail: jg201@cam.ac.uk; wzhou@st-andrews.ac.uk; bjohnson@freenet.co.uk

Abstract: Exceptionally long C_{60} nanowires, with a length to width aspect ratio as large as 3000, are grown from a 1,2,4-trimethylbenzene solution of C_{60}. They have been formed to possess a highly unusual morphology, with each nanowire being composed of two nanobelts joined along the growth direction to give a V-shaped cross section. The crystal structure of these nanowires is found to be orthorhombic, with the unit cell dimensions of $a = 10.2$ Å, $b = 20.5$ Å, and $c = 25.6$ Å. Structural and compositional analyses enable us to explain the observed geometry with an anisotropic molecular packing mechanism that has not been observed previously in C_{60} crystal studies. The nanowires have been observed to be able to transform into carbon nanofibers following high-temperature treatment, but the original V-shaped morphology can be kept unchanged in the transition. A model for the nanowire morphology based upon the solvent−C_{60} interactions and preferential growth directions is proposed, and potentially it could be extended for use to grow different types of fullerene nanowires.

1. Introduction

The carbon skeleton of a C_{60} molecule is a truncated icosohedron with 20 hexagons and 12 pentagons, and the nuclear framework diameter is 7.1 Å. The growth of fullerene (C_{60}) crystals has been of considerable scientific and technological interest.[1,2] Among the various crystalline forms, C_{60} nanowires are of particular interest because of the properties associated with their high surface area, low-dimensionality, and potential quantum confinement effect,[3,4] as well as serving as 1D building blocks in future magnetic or photonic applications.[5,6] Prior research on the growth of C_{60} crystals may be broadly split into two main themes. The first has concentrated on the utilization of the low sublimation temperature (~600 °C) of solid C_{60} to grow millimeter-size single crystals which exhibit prominent crystalline facets.[7] This vapor growth method is of historical importance because the crystals obtained allow for the determination of the intrinsic structure, a face-centered cubic (fcc) lattice.[8−10] This cubic fullerene undergoes an orthorhombic distortion at low temperatures to give the optimal structure in which the orientation of C_{60} molecules is such that each C_{60} has eight substantial interactions of its hexagonal rings with the neighboring molecules.[11,12] However, at near room temperatures (300−400 K), transformation from one favored orientation to another occurs. Such orientation changes lead to an average fcc structure with the unit cell of $a = 14.13$ Å at 300 K, and orientation disordering is observed.[8−14] No wire-like 1D single crystals have been obtained by this vapor deposition technique presumably because the simple cubic lattice allows the crystals to grow relatively evenly on each of their facets.

In the second area, research has focused on using saturated organic solvents for the crystal growth. Incorporation of solvent molecules into the crystal lattices leads to different crystalline forms including needle-like C_{60} crystals.[15−28] The volume of the unit cell has been demonstrated to increase with the increase of the molecular size of the solvents. For example, an increment of approximately 17 Å^3 was observed for each additional CH_2 group in the *n*-alkane solvent series,[16,29] suggesting that the solvent has been incorporated into the crystal lattices. These

† Department of Chemistry, University of Cambridge.
‡ School of Chemistry, University of St. Andrews.
§ Department of Materials Science and Metallurgy, University of Cambridge.

(1) Kratschmer, W.; Lamb, L. D.; Fostiropoulos, K.; Hoffman, D. R. *Nature* **1990**, *347*, 354.
(2) Stephens, P. W.; Mihaly, L.; Lee, P. L.; Whetten, R. L.; Huang, S. M.; Kaner, R.; Diederich, F.; Holczer, K. *Nature* **1991**, *351*, 632.
(3) Dresselhaus, M. S.; Dresselhaus, G.; Eklund, P. C. *Science of Fullerenes and Carbon Nanotubes*; Academic Press: San Diego, CA, 1996.
(4) Lieber, C. M.; Wang, Z. L. *MRS Bull.* **2007**, *32*, 99.
(5) Guss, W.; Feldmann, J.; Gobel, E. O.; Taliani, C.; Mohn, H.; Muller, W.; Haubler, P.; ter Meer, H. U. *Phys. Rev. Lett.* **1994**, *72*, 2644.
(6) Saito, R.; Dresselhaus, G.; Dresselhaus, M. S. *Phys. Rev. B* **1992**, *46*, 9906.
(7) Fleming, R. M.; Siegriest, T.; Marsh, P. M.; Hessen, B.; Kortan, A. R.; Murphy, D. W.; Haddon, R. C.; Tycko, R.; Dabbagh, G.; Mujsce, A. M.; Kaplan, M. L.; Zahurak, S. M. *Mater. Res. Soc. Symp. Proc.* **1991**, *206*, 691, Materials Research Society Press, Pittsburgh.
(8) Kortan, A. R.; Kopylov, N.; Glarum, S. H.; Gyorgy, E. M.; Ramirez, A. P.; Fleming, R. M.; Thiel, F. A.; Haddon, R. C. *Nature* **1992**, *355*, 529.
(9) Li, Z. G.; Fagan, P. J. *Chem. Phys. Lett.* **1992**, *194*, 461.
(10) de Boer, J. L.; van Smaalen, S.; Petricek, V.; Dusek, M.; Verheijen, M. A.; Meijer, G. *Chem. Phys. Lett.* **1994**, *219*, 469.
(11) Guo, Y. J.; Karasawa, N.; Goddard, W. A., III. *Nature* **1991**, *351*, 464.
(12) Tycko, R.; Haddon, R. C.; Dabbagh, G.; Glarum, S. H.; Douglas, D. C.; Mujsce, A. M. *J. Phys. Chem.* **1991**, *95*, 518.
(13) Heiney, P. A.; Fischer, J. E.; McGhie, A. R.; Romanow, W. J.; Denestein, A. M.; McCauley, J. P.; Smith, A. B.; Cox, D. E. *Phys. Rev. Lett.* **1991**, *66*, 2911.
(14) Miyazaki, Y.; Sorai, M.; Lin, R.; Dworkin, A.; Szwarc, H.; Godard, J. *Chem. Phys. Lett.* **1999**, *305*, 293.

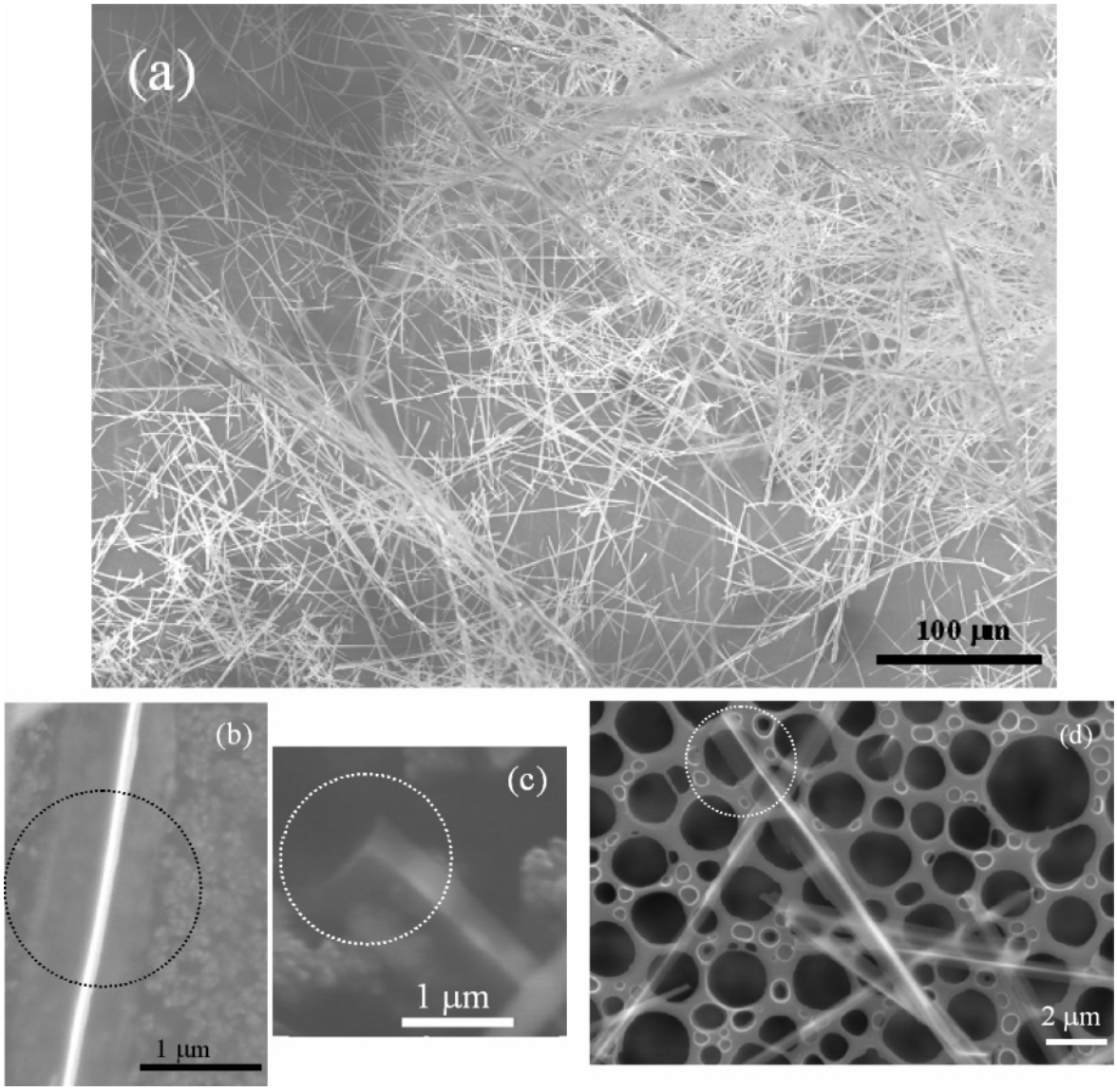

Figure 1. SEM and TEM images of the C_{60} nanowires. (a) A low magnification SEM image to show the overall morphology of the nanowires. (b) A magnified SEM image of a single nanowire with the crystal ridge facing up, to show the two component nanobelts along the crystal ridge. (c) A SEM image to show the V-shaped end (The cross section, see the marked circle area) of the nanowire together with the crystal ridge. (d) A TEM image to show the V-shaped cross section and the two component nanobelts within each nanowire. As the nanobelts are thin and transparent, the holey carbon supporting film beneath the nanowires can be clearly seen under the e-beam. The marked circle area shows a nanowire with the crystal ridge facing up at one end and thus displaying an inverse V-shaped cross section.

needle-like crystals are usually quite large (0.1 to 1 mm wide, 5 to 20 mm long), and consequently the length-to-width ratio is rather short (typically around 10, although in some cases this ratio may reach ~20). Recently, C_{60} nanowhiskers have been prepared by using a "liquid−liquid interfacial precipitation" method.[30−33] Unfortunately, the nature of the interactions between C_{60} and the solvent is not known, and the structure of these nanowhiskers has not been determined because of the lack of detailed knowledge of these fullerene crystals. The growth mechanism remains unclear at present. We have investigated the growth of C_{60} crystals in order to ascertain more detailed information of the relationship between growth and structure. Here we report that unusually long crystalline C_{60} nanowires can be grown using 1,2,4-trimethylbenzene (1,2,4-TMB) as solvent. The crystal structure and the chemical composition have been identified, which enables us to address an important fundamental question of how these C_{60} molecules grow into nanowires with the observed morphology.

(15) Fleming, R. M.; Kortan, A. R.; Hessen, B.; Siegriest, T.; Thiel, F. A.; Marsh, P. M.; Haddon, R. C.; Tycko, R.; Dabbagh, G.; Kaplan, M. L.; Mujsce, A. M.; Zahurak, S. M. *Phys. Rev. B* **1991**, *44*, 888.
(16) Toscani, S.; Allouchi, H.; Tamarit, J. L1; Lopez, D. O.; Barrio, M.; Agafonov, V.; Rassat, A.; Szwarc, H.; Ceolin, R. *Chem. Phys. Lett.* **2000**, *330*, 491.
(17) Kawada, H.; Fujii, Y.; Nakao, H.; Murakami, Y.; Watanuki, T.; Suematsu, H.; Kikuchi, K.; Achiba, Y.; Ikemoto, I. *Phys. Rev. B* **1995**, *51*, 8723.
(18) Michaud, F.; Barrio, M.; Toscani, S.; Lopez, D. O.; Tamarit, J. L.; Agafonov, V.; Szwarc, H.; Ceolin, R. *Phys. Rev. B* **1998**, *57*, 10351.
(19) Kikuchi, K.; Suzuki, S.; Saito, K.; Shiromaru, H.; Ikemoto, I.; Achiba, Y.; Zakhidov, A. A.; Ugawa, A.; Imaeda, K.; Inokuchi, H.; Yakushi, K. *Physica C* **1991**, *185−189*, 415.
(20) Ceolin, R.; Tamarit, J. L1.; Lopez, D. O.; Barrio, M.; Agafonov, V.; Allouchi, H.; Moussa, F.; Szwarc, H. *Chem. Phys. Lett.* **1999**, *314*, 21.
(21) Ceolin, R.; Agafonov, V.; Fabre, C.; Rassat, A.; Dworkin, A.; Andre, D.; Szwarc, H.; Schierbeek, A. J.; Bernier, P.; Zahab, A. *J. Phys. I (France)* **1992**, *2*, 1.
(22) Michaud, F.; Barrio, M.; Toscani, S.; Agafonov, V.; Szwarc, H.; Ceolin, R. *Fullerene. Sci. Technol.* **1997**, *5*, 1645.

2. Experimental Section

A solution of C_{60} in 1,2,4-TMB with a concentration of 2×10^{-3} M was employed for growth of the nanowires using C_{60} powder with a high purity (99.9%, SERS Ltd.). The solution was aged in a glass vial at room temperature. The vial was loosely covered with a plastic plate on the top. For every 2 or 3 days, the vial was rotated for a while so that the solution could repeatedly rinse its internal glass wall. The vaporization rate of the solvent was observed to be extremely slow, which was indicated by a just noticeable level drop of the solvent for over 3 weeks and the solution not drying until 6 months later. Following the slow vaporization of the solvent, an abundant growth of cotton-like nanowires was found on the upper internal wall and around the mouth area of the container. The nanowires have a golden brown color. Apart from these very thin and long nanowires, a small amount of much larger, needle-like C_{60} crystals, with a dark brown to black color and a width of ~0.5−1.0 mm and a length of ~5−15 mm, were also found at the lower part of the container.[34] The obtained nanowires are found to be extremely stable in air. There is no spontaneous decomposition that can be observed in air storage for over a year.

Scanning electron microscopic (SEM) images were obtained from both the JSM-5600 scanning electron microscope operated at 15 to 20 kV and the LEO-32 electron microscope operated at 5 kV. Samples were directly deposited on a specimen holder (carbon mat) without surface coating of a conducting material. High-resolution transmission electron microscopic (HRTEM) images were recorded with a Gatan 794 CCD camera on a JEOL JEM-2011 electron microscope operated at 200 kV. To prepare a specimen for the TEM study, a C_{60} sample was ground in acetone to make a suspension. One drop of the suspension was then deposited on a copper specimen grid coated with a holey carbon film. The specimen grid was then placed in a double tilt specimen holder and transferred into the microscopic column. To reduce the electron beam damage, a very low beam irradiation dose, e.g., <2 pA/cm^2, was applied. Chemical composition of the specimen was examined by energy dispersive X-ray microanalysis (EDX) for detecting any other possible heavy elements. Selected area electron diffraction (SAED) was used to determine the unit cell.

Gas chromatography followed by the mass spectroscopic analyses (GC−MS) was carried out on a Perkin-Elmer Turbomass GCMS system using the splitless injection technique. This system utilizes an Auto-system XL GC connected to a small quadrupole mass analyzer. The GC was performed with an injection temperature of 200 °C, an injection volume of 0.5 and 1 μL, a helium carrier gas pressure of 40 psi, and a Perkin-Elmer Elite PE-5MS column composed of 5% phenyl and 95% methyl polysiloxane. The splitless mode of injection allows the entire sample from an injection to be analyzed and is a suitable technique for samples of low concentration. The mass analysis was done by using the EI+ ionization mode, an ionization energy of 70 eV, a transfer line temperature of 200 °C, and the mass range scanned at 50−650 Da.

The Raman studies were performed using a microspectrometer with the Renishaw software. The wavelength of the incident Ar ion laser was λ = 514.5 nm. Thermal gravimetrical analysis (TGA) was performed in argon (Ar) using a TGA/SDTA 851e system with STAR^e software. The rate at which temperature was increased was set at 5 °C/min, and the Ar flow rate, at ~130 cm^3/min. The microbalance resolution is 1 μg.

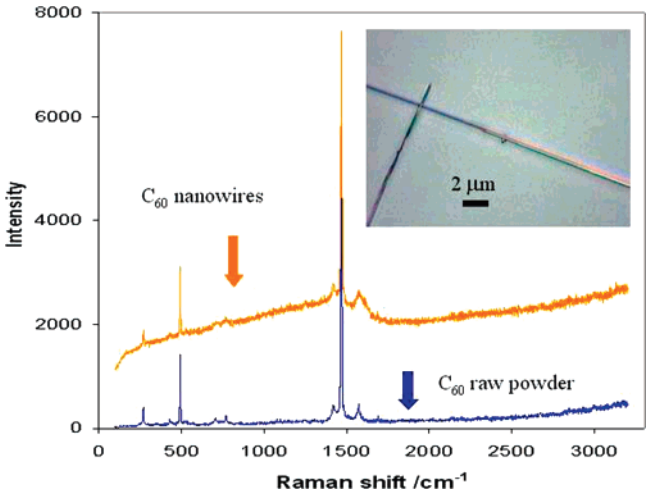

Figure 2. Laser Raman spectroscopic profiles of the C_{60} nanowires and the raw C_{60} powder. The inset shows a typical optical image of the nanowires used for the Raman measurements.

3. Results and Discussion

Nanowire Morphology and Structure. Examinations of the grown C_{60} nanowires by both SEM and TEM indicate that they are typically 100 to 500 nm wide, 200 to 1000 μm long, with some wires as long as ~1.5 mm. The length to width aspect ratio is thus estimated to be up to 3000. Close inspection using the electron microscopy shows that these nanowires possess a highly unusual morphology, with each being composed of two nanobelts joined along the growth direction to give a V-shaped cross section, and each nanobelt is only up to a few tens of nanometers thick (Figure 1).

Micro-Raman spectroscopy (Ar^+ ion excitation laser at λ = 514 nm, spot size of ~10 μm) was performed to investigate the isolated C_{60} molecules within the nanowires (Figure 2). Extra care was taken to ensure that the employed laser intensity was as low as possible in order to prevent photoinduced damage to the sample (with high laser powers the crystals were observed to transform into graphitic carbon). As in the case of the initial C_{60} powder, the two Raman A_g modes of the first-order scatterings were clearly observed, with the expected positions at 1468 and 490 cm^{-1}, respectively. A number of active H_g modes such as the bands of 271, 425, 700, 768, 1229, 1417, and 1571 cm^{-1} were also observed. The appearance of these A_g and H_g modes and also the lack of the band at 1458 cm^{-1} indicate that the C_{60} in the crystal lattice are pristine molecules. No polymerization has occurred in the lattice because such polymerization would cause an abrupt shift of the band of 1468 cm^{-1} to 1458 cm^{-1}, and the latter has been frequently accepted as a signature for identifying the formation of the C_{60} polymers with the [2 + 2] cycloaddition structure.[35,36]

The crystalline structure of the C_{60} nanowires was investigated by using high-resolution TEM (HRTEM). The specimen was found to be electron beam sensitive. Intensive or prolonged exposure to the beam can cause decomposition of the sample.

(23) Ceolin, R.; Agafanov, V.; Moret, R.; Fabre, C.; Rassat, A.; Dworkin, A.; Andre, D.; Szwarc, H.; Schierbeek, A. J.; Bernier, P.; Zahab, A. *Carbon* **1992**, *30*, 1121.
(24) Hawkins, J. M.; Lewis, T. A.; Loren, S. D.; Meyer, A.; Heath, J. R.; Saykally, R.; Hollander, F. J. *J. Chem. Soc., Chem. Commun.* **1991**, 775.
(25) Meidine, M.; Hitchcock, P. B.; Kroto, H. W.; Tylor, R.; Walton, D. R. M. *J. Chem. Soc., Chem. Commun.* **1992**, 1534.
(26) Balch, A. L.; Lee, J. W.; Noll, B. C.; Olmstead, M. M. *J. Chem. Soc., Chem. Commun.* **1993**, 56.
(27) Burgi, H. B.; Restori, R.; Schwartzenbach, D.; Balch, A. L.; Lee, J. W.; Noll, B. C.; Olmstead, M. M. *Chem. Mater.* **1994**, *6*, 1325.
(28) Yosida, Y.; Arai, T.; Suematsu, H. *Appl. Phys. Lett.* **1992**, *61*, 1043.
(29) Kitaigorodskii, A. I. *Organic Crystal Chemistry*; Consulants Bureau: New York, 1961; pp 12−17.
(30) Miyazawa, K.; Nishimura, C.; Fujino, M.; Suga, T.; Yoshii, T. *Trans. Mater. Res. Soc. Jpn.* **2004**, *29*, 1965.
(31) Yosida, Y. *Jpn. J. Appl. Phys.* **1992**, *31*, 505.
(32) Miyazawa, K.; Suga, T. *J. Mater. Res.* **2004**, *19*, 3145.

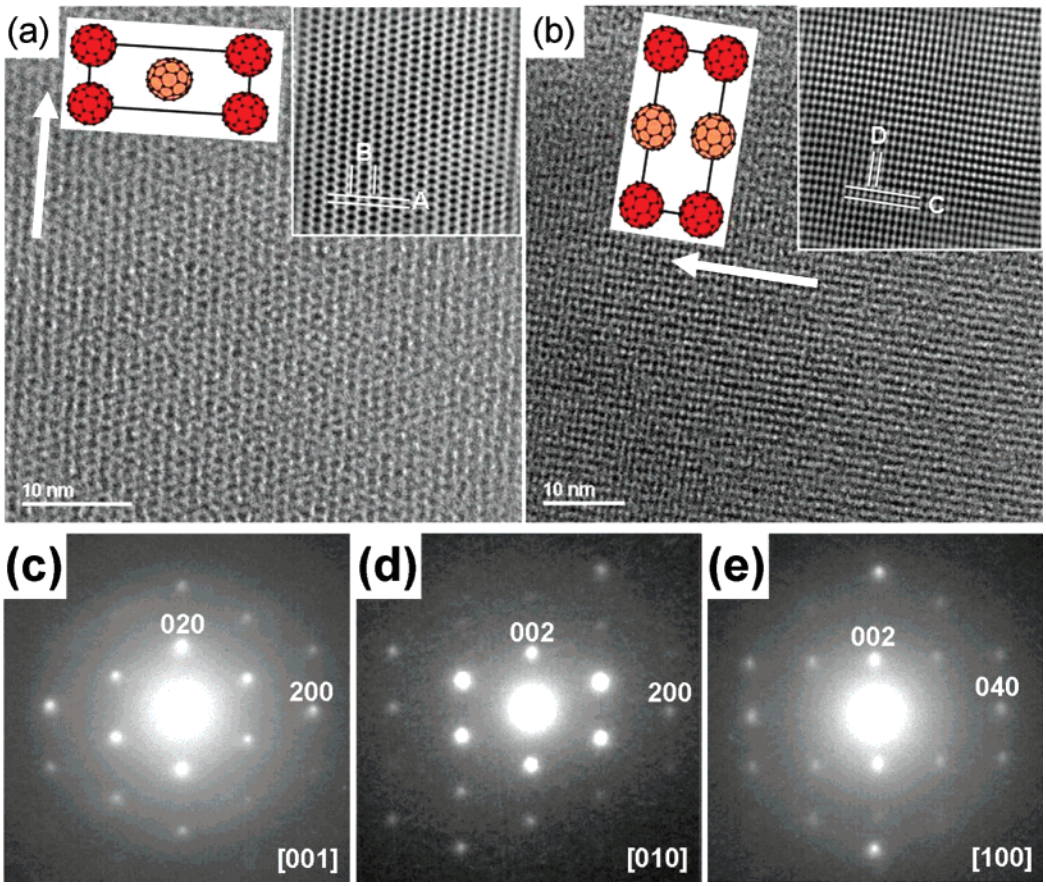

Figure 3. Electron microscopy of the C_{60} nanowires. (a and b) HRTEM images of the nanowires on the [010] and [100] projection, respectively. The insets in (a) and (b) are computer-created corresponding images after removing the background noise (right corners), and the corresponding projections of the structure (colored C_{60} molecules). The *d*-spacings are indicated by using the A (100), B (001), C (002), and D (020) planes. The arrows indicate the nanowire growth directions. (c, d, and e) SAED patterns viewed down the [001], [010], and [100] zone axis of the orthorhombic unit cell, respectively.

In this work, successful acquisition of the good selected area electron diffraction (SAED) patterns and the reasonably ordered lattice images was achieved by controlling the beam brightness, for example, by applying a very low irradiation dose such as <2 pA/cm^2. This method has been successfully used in our previous studies of other beam sensitive materials, such as zeolites.[37] Figure 3a and b are the HRTEM images of the C_{60} crystal lattices viewed on the projections of [010] and [100], and Figure 3c, d, and e, the SAED patterns recorded down the [001], [010], and [100] directions, respectively. The measured *d*-spacings are as follows: $d(010) = 20.5$ Å, $d(100) = 10.2$ Å (from Figure 3c); $d(002) = 12.8$ Å, $d(200) = 5.11$ Å (from Figure 3d); $d(002) = 12.2$ Å, $d(020) = 10.3$ Å (from Figure 3e). Based on these measurements, a hitherto unreported unit cell, an orthorhombic structure with the cell dimensions of $a = 10.2$ Å, $b = 20.5$ Å, and $c = 25.6$ Å was revealed.

Figure 4a shows the basic packing arrangement of the C_{60} molecules in the half unit cell, $a \times 0.5b \times c$, derived from the whole cell. In this structure, C_{60} forms a pseudo-square pattern on the (*ab*) plane with an intermolecular distance of 10.2 Å. This is approximately the same distance as normally found in a fcc C_{60} lattice. However, the molecules in the neighboring layer are two instead of four C_{60} molecules. The measured intermolecular distance between these two layers is about 13.8 Å, which is significantly larger than the normal $C_{60}-C_{60}$ distance. Consequently, it is reasonable to believe that there are other chemical ions or molecules fully or partially occupying the positions marked by the white balls. These unknown guest ions/molecules may cause lattice distortion, leading to the formation of the $1 \times 2 \times 1$ superstructure as shown by the basic cell of Figure 4a.

Chemical Composition. In order to identify the unknown guest species, the specimen was first examined by EDX which detected the only element, carbon. These "missing species" in the unit cell are then believed to be the 1,2,4-TMB molecules employed as solvent for the crystal growth. To test this hypothesis, the nanowires were dissolved in carbon tetrachloride (CCl_4) and the chemical composition was determined by GC−MS (gas chromatography followed by mass spectroscopic measurement). By these means, we have successfully identified

(33) Tachibana, M.; Kobayashi, K.; Uchida, T.; Kojima, K.; Tanimura, M.; Miyazawa, K. *Chem. Phys. Lett.* **2003**, *374*, 279.
(34) Both types of the crystals were found at positions above the initial level of the solution, suggesting that the nucleation occurred on the glass wall rather than inside the solution. In contrast to the nanowires which have grown into random orientations and the whole bulk phase tended to extrude toward the central space of the vial, those much larger needle-like crystals vertically place themselves along the cylindrical wall with their smaller and thus sharper ends pointing downwards.
(35) Rao, A. M.; Zhou, P.; Wang, K. A.; Hager, G. T.; Holden, J. M.; Wang, Y.; Lee, W. T.; Bi, X. X.; Eclund, P. C.; Cornett, D. S.; Duncan, M. A.; Amster, L. J. *Science* **1993**, *259*, 955.
(36) Eklund, P. C.; Rao, A. M.; Zhou, P.; Wang, Y.; Holden, J. M. *Thin Solid Films* **1995**, *257*, 185.
(37) (a) Wright, P. A.; Zhou, W. Z.; Perez-Pariente, J.; Arranz, M. *J. Am. Chem. Soc.* **2005**, *127*, 494. (b) Chen, X. Y.; Qiao, M. H.; Xie, S. H.; Fan, K. N.; Zhou, W. Z.; He, H. Y. *J. Am. Chem. Soc.* **2007**, *129*. 13305.

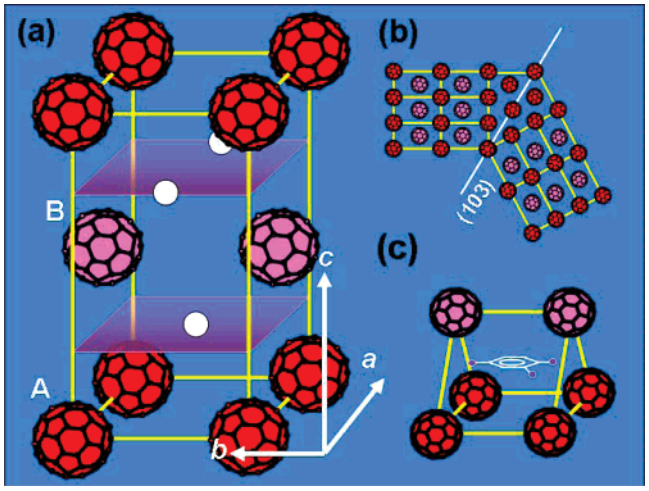

Figure 4. The structure shows the molecular packing of C_{60}/1,2,4-TMB in the unit cell. (a) The arrangement of C_{60} in a half unit cell, $a \times 0.5b \times c$. A and B indicate two C_{60} layers separated by the trimethylbenzene molecules at the positions of white balls. (b) A schematic drawing to show the formation of the twin crystallization in the nanowires. (c) A schematic drawing to show the coordination of each trimethylbenzene molecule surrounded by six C_{60} molecules.

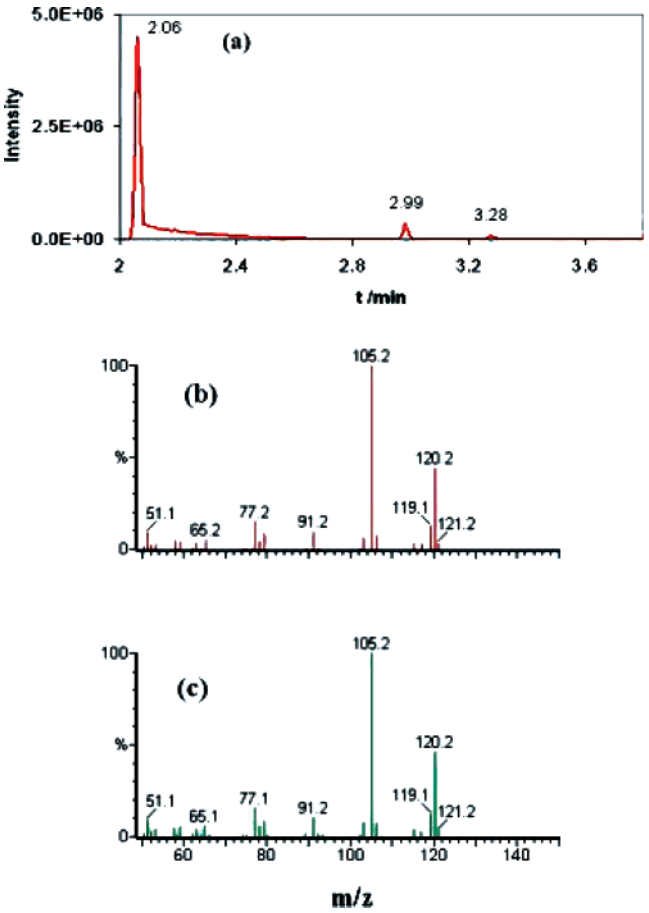

Figure 5. GC−MS analysis of the chemical composition of the C_{60} nanowires. (a) The GC result from the dissolved sample in CCl_4. (b and c) The mass spectra of the components isolated by GC and labeled by the peaks 2.99 and 3.28 in (a), respectively.

three components, as indicated by the three GC peaks shown in Figure 5a. The peak labeled at 2.06 min is due to the remnants of the CCl_4 from the injection. The peaks at 2.99 and 3.28 min both show similar mass spectra with major ions at 120.2 Da

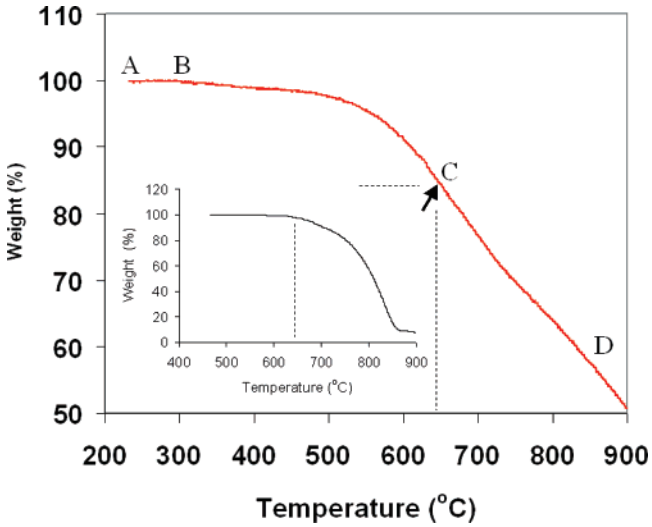

Figure 6. TGA analysis of the C_{60} nanowires with a rate of temperature increase of 5 °C/min in argon. The inset is a result from the raw C_{60} powder with a high purity of 99.9%

(Figure 5b and c), which are consistent with the ions expected from trimethylbenzene. The presence of the two GC peaks suggests that two forms of the molecular isomers (one is 1,2,4-TMB, and another small peak corresponds to either 1,3,5-TMB or 1,2,3-TMB as the impurity involved in the solvent) are detected. Another large mass peak at 105.2 arises from the molecular fragments of trimethylbenzene after eliminating a $-CH_3$ group in the electron ionization chamber. These analytical results unambiguously indicate that the nanowires contain 1,2,4-TMB molecules within their crystal lattices, which agrees with our aforementioned structural analysis by HRTEM and the electron diffraction patterns.

The ratio of the 1,2,4-TMB to C_{60} was determined by thermal gravimetric analysis (TGA) performed in an argon atmosphere. The removal of the guest/solvent molecules from the crystals is expected to occur at lower temperatures, and this process should be followed by the sublimation of the solid C_{60} at higher temperatures. However, in this case the two weight-loss processes cannot be clearly separated in the observed TGA curve. As can be seen from Figure 6, the sample starts to lose weight at a temperature of ~300 °C and the weight loss continues until the maximum temperature of the experiment is reached (900 °C). There is no clear boundary between the two processes, suggesting that the removal of the guest species overlaps with the C_{60} sublimation process. It is therefore necessary to perform the TGA for a pure C_{60} sample under identical experimental conditions. For this reference purpose, the TGA test for the raw C_{60} powder (a dried sample with a high purity of 99.9%) was performed and the result showed that this material starts the sublimation at ~ 644 °C (see the inset of Figure 6). Using this temperature as a reference point, we have roughly separated the above-mentioned two processes, that is to say, the weight loss before this temperature is mainly attributed to the removal of the solvent from the solid and after the temperature to the sublimation of the C_{60}. Close inspection of the TGA curve also indicates that this temperature is in coincidence with a turning point on the curve, which appears to further support the above view. By this means we have estimated that the weight percentage of the 1,2,4-TMB in the sample is ~14.7 wt % and accordingly, the C_{60} content is ~85.3

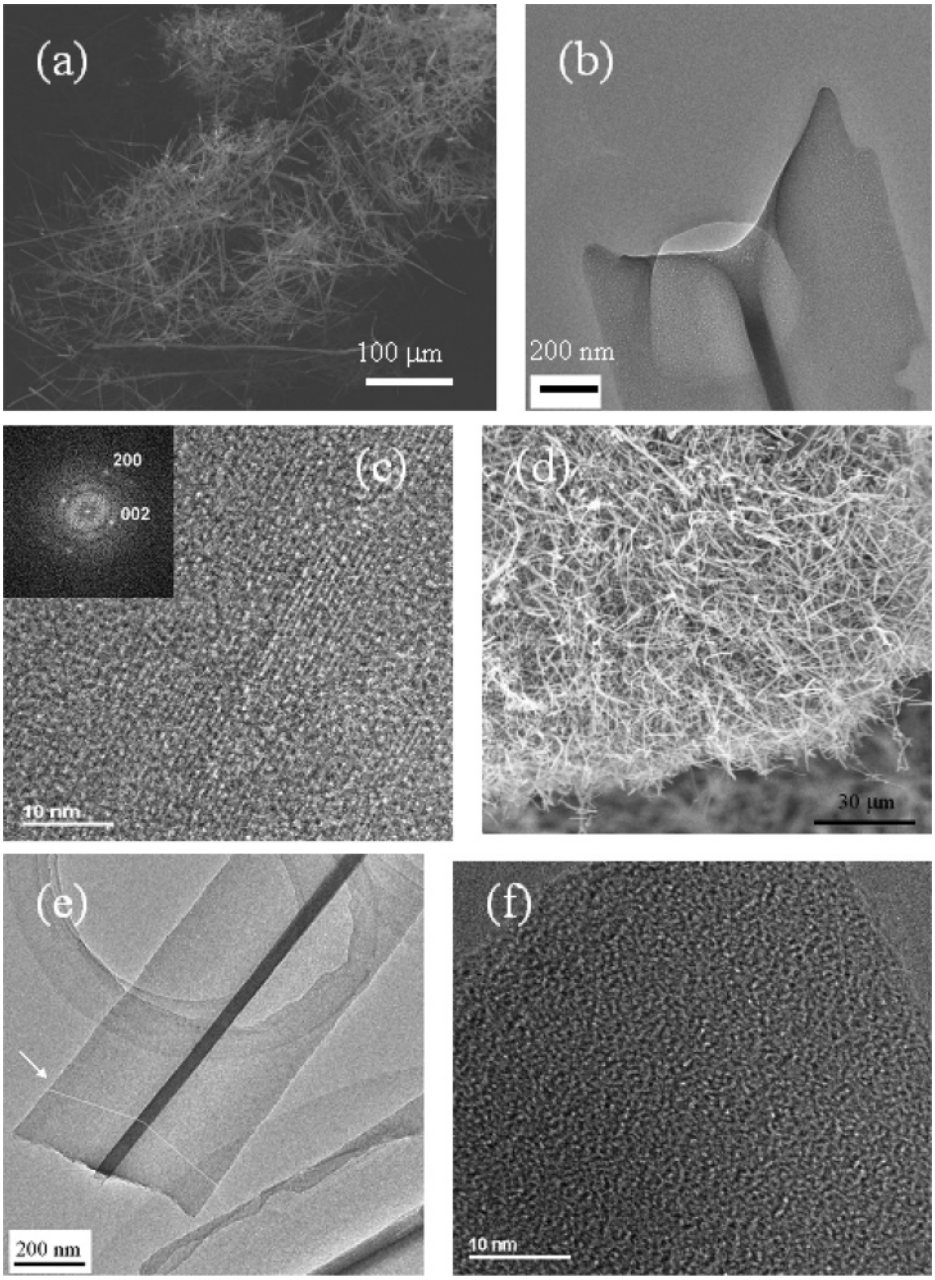

Figure 7. Electron microscopic observations of the heat-treated C_{60} nanowires and their transformation from the crystalline structure to carbon nanofibers. (a−c) Images of the nanowires after heat treatment to 440 °C. (a) A SEM image. (b) A TEM image to indicate that the characteristic V-shaped morphology remains after the heat treatment. (c) An HRTEM image to show the crystalline structure has been retained in the heated sample. (d−f) Images of the carbon nanofibers formed from the transformation of the nanowires after heat treatment to 900 °C. (d) An SEM image. (e) A TEM image to show the unchanged morphology. (f) An HRTEM image to show the disordered carbon microstructure in the nanofiber.

wt % (Figure 6). This estimated relative weight percentages may be converted into the molar ratio of the organic molecules to the fullerene, which is ∼1:1. These data support our previous speculation based upon the HRTEM observation of the crystalline structure and the measurement of the dimensions of the unit cell that, for each void formed from six adjacent C_{60} molecules in the unit cell, the space may be used to accommodate one 1,2,4-TMB molecule (Figure 4c).

TGA analyses for both the raw C_{60} powder and the C_{60} nanowires indicate that there is a considerable amount of fullerene that cannot sublimate but remains as residue at temperatures up to 900 °C (for the raw C_{60}, this residue accounts for ∼10 wt % of the initial sample weight; for the nanowires, this value has increased to ∼51 wt %). This observation is consistent with the literature reports about the partial sublimation of C_{60} at elevated temperatures.[3,38,39]

Transformation into Carbon Nanofibers. Somewhat to our surprise, the original shape and morphology of these C_{60} nanowires have remained unaffected after heat treatment in argon with temperatures as high as 900 °C (the maximum temperature in this experiment). For one test, the nanowire sample was first heated at 200 °C for ∼20 min and then at 350 °C for an extended time (>3 h) to drive off most of the residual solvent followed by a further annealing at 440 °C for

(38) Verheijen, M. A.; Meekes, H.; Meijer, G.; Bennema, P.; de Boer, J. L.; van Smaalen, S.; Tendeloo, G. V.; Amelinckx, S.; Muto, S.; van Landuyt, J. *Chem. Phys.* **1992**, *166*, 287.
(39) Verheijen, M. A.; Meekes, H.; Meijer, G.; Raas, E.; Bennema, P. *Chem. Phys. Lett.* **1992**, *191*, 339.

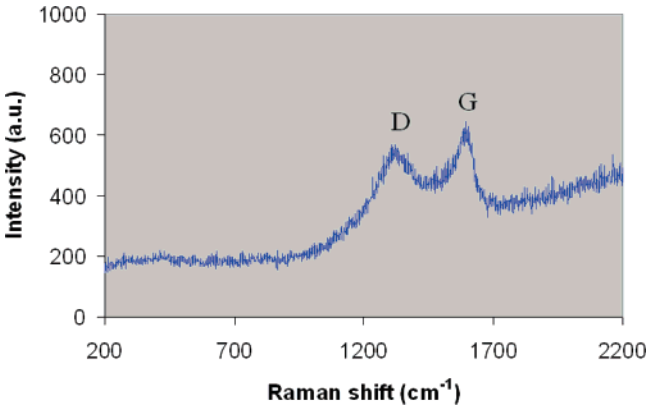

Figure 8. Laser Raman test of the carbon nanofibers formed from the transformation of the C_{60} nanowires. In this test, the wavelength of the incident laser is 633 nm.

1 h. Based on the above TGA analysis, it is estimated that after such a lengthy period of heat treatment, the 1,2,4-TMB molecules should be considerably, if not fully, removed from the crystalline lattice. We observed that there was a color change associated with the heat treatment, which was indicated by the color evolution from the original golden yellow to a dark brown. Examination of the heated sample by SEM, however, shows that the original 1D shape was retained (Figure 7a), and TEM observation also shows the unchanged morphology characterized by the component nanobelts and the V-shaped cross section (Figure 7b). Well oriented crystalline domains could still be observed by HRTEM imaging and the SAED patterns, although in some areas damage or partial decomposition of the crystals occurred (Figure 7c). More interestingly, the unit cell dimension along the [100] zone axis stays the same as observed before (10.2 Å), while the *c* dimension is greatly compressed from 25.6 to 17.4 Å. This compression is attributed to the removal of the organic molecules from the crystals and the resultant shrinking of the C_{60} structure along the *c*-axis. However, the edge-centered symmetry remains unchanged. If we consider the smallest $C_{60}-C_{60}$ distance to be $a = 10.2$ Å, which is adopted in the new structure, the ideal *c* dimension would be $\sqrt{3}a = 17.7$ Å, a value very close to that measured in this test.

The heat treatment at higher temperatures resulted in transformation of the nanowires to carbon nanofibers. This was observed by heating the sample to 900 °C under a rate of temperature increase of 5 °C/min and examining the heated sample by SEM and TEM (Figure 7d−f). Following this heat treatment, the original crystalline structure was lost and a new disordered carbon microstructure was found (HRTEM, Figure 7f). The laser Raman test is consistent with the HRTEM observation (Figure 8). The initially observed Raman active modes of A_g and H_g for pristine C_{60} molecules have disappeared, and these are now replaced by the characteristic D (Defective, 1315 cm^{-1}) and G (Graphitic, 1585 cm^{-1}) peak for noncrystalline carbon with the D to G ratio of about 1:1.[40] Nevertheless, the original 1D shape and the V-shaped morphology have persisted in the transition (Figure 7d and e). This is interesting because such an observation appears to have provided a novel way of making carbon nanofibers by the transformation of C_{60} nanowires. Compared with the widely used CVD (chemical vapor deposition) method for growing carbon nanofibers, an advantage of this new approach is that it does not require a metal catalyst. As a consequence, the normally employed postgrowth purification for removing the metal is no longer necessary.

Growth Mechanism. One fundamentally important question is why the fullerene grows into nanowires with the observed morphology. To address this, we would first stress that the organic solvent plays an important role. The introduction of the solvent as a guest species leads us to believe that a prior solvation to the C_{60} molecules occurs before the crystals grow. This is rationalized by considering the high boiling point of the 1,2,4-TMB, ~168 °C, and also its high solubility to C_{60}, 33.5×10^{-4} M at 298 K.[41] The high boiling point tends to lead to a slow solvent vaporization. The high solubility implies that the solvent has a high chemical affinity to the fullerene presumably because of the strong interactions between their π-aromatic rings. As the consequence, significant solvation to C_{60} is expected to occur. This view is also supported by our observation that no crystals were formed at the bottom of the vessel. All nanowires were found at the upper wall and around the mouth area of the container, with some nanowires on top of the others. The whole solid phase extends toward the center of the container. This phenomenon indicates that the crystal growth is different from the conventional process where a supersaturated solution tends to yield crystals at the bottom of the vessel. In the current work, the C_{60} molecules diffused with the solvent along the glass wall up to the mouth area of the container, where the solvent vaporized and went away but left the C_{60} to nucleate.

The observed nanowire morphology demonstrates that the growth of these wires requests the molecules to be packed in a way that their stacking is significantly orthorhombically distorted away from the intrinsic fcc structure of C_{60}. We propose a molecular anisotropic packing mechanism to explain this phenomenon based on the solvent effect. Growth may occur along either the [010] or the [100] axis but with the most growth occurring along the [010] direction (Figure 3a and b). Although the C_{60} molecules may pack directly on both of the (100) and (010) surfaces, the molecular densities on these two surfaces are different. Compared with the only 1 molecule per unit cell on the (100) surface, there are 2 molecules per unit cell on the (010) surface (see Figure 4a). According to the Hartman−Perdok approach to the geometrical theory of crystal growth,[42] the growth on the (010) surface should be more favored and the growth rate is therefore faster than that on the (100) surface.

The formation of the C_{60} nanowires may be explained from the commonly found twin crystallization phenomenon, and in this case, it is rationalized by the proposed model as shown in Figure 4b. The twin plane is parallel to the (103) plane of the unit cell. Accordingly, the twin angle is estimated to be in the range 110°−120°. In the twin area the occupation density of the organic guest species may be smaller compared with that of the bulk nanobelts. Consequently, a higher image contrast pattern on the twin boundaries is expected due to the domination of diffraction contrast, and this is confirmed by the TEM observations. The structural studies allow us to believe that the

(40) Geng, J.; kinloch, I. A.; Sing, C.; Golovko, V. B.; Johnson, B. F. G.; Shaffer, M. S. P.; Li, Y.; Windle, A. H. *J. Phys. Chem. B* **2005**, *109*, 16665.
(41) Kadish, K. M., Ruoff, R. S., Eds. *Fullerene, chemistry, physics and technology*; John Wiley & Sons, Inc.: 2000.
(42) Hartman, P.; Perdok, W. G. *Acta Crystallogr.* **1955**, *8*, 49−52; 521−524; 525−529.

crystal growth starts from this area, and its formation along the 1D dimension as the crystal ridge serves as a nucleation place for the subsequent growth of the two nanobelts as two wings of the ridge. In this case, the nanobelt thickness is determined by the size of the twin area, i.e., the width of the crystal ridge as observed in the TEM images. The growth of these nanobelts along all their three zone axes of [100], [010], and [001] may simultaneously take place. However, different from the molecular packing along the directions of [010] and [100], the growth along the [001] zone axis is controlled by the alternative packing of the C_{60} and 1,2,4-TMB layers. This novel mechanism of nucleation and growth explains why the observed nanowires possess two symmetrical flat portions associated with the crystal ridge. It also suggests that the overall 1D growth rate of a nanowire would depend on the nucleation rate of the corresponding crystal ridge along the growth direction.

4. Conclusions and Perspectives

We have demonstrated that exceptionally long C_{60} nanowires with a length to width aspect ratio as large as 3000 can be grown from a 1,2,4-trimethylbenzene solution of C_{60}. To our knowledge, this is the first report on the growth of such a 1D fullerene that is composed of two nanobelts joined along the growth direction and thus shows a highly unusual V-shaped cross section resembling the V-shaped Girder steel frequently used in building industries. The identification of the crystal structure and chemical composition has provided useful insights into the growth mechanism involving the interactions between the fullerene and the organic molecules. We also show that these fullerene nanowires may transform into carbon nanofibers following a high-temperature treatment, but their original shape can be kept unchanged through the transition. This interesting phenomenon may offer a method of making carbon nanofibers with a morphology inherited from their nanowire precursors but without using a metal as the growth catalyst, something of considerable value for carbon nanotechnology.

As can be seen from this work, the growth of these C_{60} nanowires is significantly orthorhombically distorted away from the intrinsic face-centered cubic crystal structure of C_{60}. Formation of such a 1D network may be realized by the inclusion of a second species into the crystal lattice. Organic molecules with a high chemical affinity to C_{60} may serve in this role owing to their possible solvation effect to the fullerene. Molecules with one or several benzene rings could be better candidates as they are aromatic and tend to have strong interactions with the aromatic rings of C_{60}. Utilization of a solvent with a high boiling point or a growth system with a confined vaporization arrangement may be considered as a bonus. Owing to the rich chemistry on the C_{60} molecular surface developed in the past decade or so, such grown fullerene nanowires could be functionalized by tethering various chemical groups onto their surface for potential applications. These nanowires might also serve as a 1D nanotemplate for preparing other inorganic nanowires. In the current work, the anomalous morphology of the nanowires also suggests that the 1,2,4-trimethylbenzene has a novel role in the regulation of the molecular packing process that leads to a preferential stacking of C_{60} molecules along different lattice planes.

Acknowledgment. J.G. is grateful for support from the European EXCELL project, W.Z.Z. thanks EPSRC for financial support and St. Andrews University for an EaStCHEM studentship for WBY, and I.A.K. thanks the Royal Academy of Engineering and the EPSRC. We also thank Dr. Bill Jones and Mr. Chris Amey (Department of Chemistry, University of Cambridge) for their assistance in TGA analysis.

JA076392S